Epitaxial growth and quantum well states study of Sn thin films on Sn induced Si(111)-($2\sqrt{3}\times 2\sqrt{3}$) *R*30° surface

L. L. Wang,[1,2] X. C. Ma,[1,*] S. H. Ji,[1] Y. S. Fu,[1] Q. T. Shen,[1] J. F. Jia,[3] K. F. Kelly,[2] and Q. K. Xue[3,1]
[1]*Institute of Physics, The Chinese Academy of Sciences, Beijing 100080, People's Republic of China*
[2]*Department of Electrical and Computer Engineering, Rice University, Houston, Texas 77005, USA*
[3]*Department of Physics, Tsinghua University, Beijing 100084, People's Republic of China*
(Received 10 October 2007; revised manuscript received 1 February 2008; published 9 May 2008)

Surface morphologies and electronic structures of Sn thin films prepared on Si(111)-Sn($2\sqrt{3}\times 2\sqrt{3}$) *R*30° substrate are investigated by low temperature scanning tunneling microscopy/scanning tunneling spectroscopy (STS). A typical Stranski–Krastanov growth is observed at various growth temperatures (95–300 K), and the Sn islands above wetting layers exhibit the preferential thicknesses of odd-numbered atomic layers. STS measurement shows the formation of well-defined quantum well states with an oscillation period of 2 ML, which modulates the surface energy and accounts for the observed preferential thicknesses. Due to the interplay between large lattice mismatch and symmetry difference, a transition from α-Sn to β-Sn occurs at 4 ML, which confirms the previous report. From 4 to 11 ML, the mismatch resulted strain manifests the growth via thickness-dependent striplike modulation structures on the surfaces of all Sn islands. Upon room temperature annealing, the as-deposited Sn islands undergo a metal-insulator transition, while the band gaps of wetting layers increase and oppositely shift with respect to the Fermi level for *n*- and *p*-type substrates. The change in electronic property is attributed to the electron transfer at the Sn-Si interface, which also affects the growth and morphologies of films.

DOI: 10.1103/PhysRevB.77.205410 PACS number(s): 68.37.Ef, 68.55.−a, 73.20.At, 68.47.Fg

I. INTRODUCTION

Sn induced surface reconstructions and phase transition on the (111) surfaces of group IV (Si and Ge) semiconductors have been extensively investigated by scanning tunneling microscopy (STM) in the past decade. In the case of 1/3 ML Sn on Ge(111), charge-density wave transition at 200 K with a structure distortion from ($\sqrt{3}\times\sqrt{3}$) *R*30° to (3×3) symmetry[1] and metal-insulator phase transition at 30 K with reverse structure distortion[2] are identified. Similar behavior on the Si(111) substrate is expected, such as a phase transition at 70 K observed by photoelectron spectroscopy.[3] In this case, besides the common metallic ($\sqrt{3}\times\sqrt{3}$) *R*30° phase induced by adsorption of 1/3 ML Sn in the fourfold atop (T_4) site,[4,5] a new semiconducting ($2\sqrt{3}\times 2\sqrt{3}$) *R*30° phase (hereafter, it is denoted as $2\sqrt{3}$ for simplification) with the first layer Sn atoms in the T_4 site and the second layer atoms in the H_3 site and total Sn coverage of 1.2 ML was reported.[5–7] The epitaxial growth at higher coverage was shown very complicated because of a phase transition from α-Sn to β-Sn,[8,9] partially due to the large lattice mismatch (~19.5%) for the α-Sn (a semiconducting phase with diamond structure, $a=6.489$ Å), partially due to the symmetry difference for the β-Sn (a metallic phase with body centered tetragonal structure, $a=5.83$ Å and $c=3.18$ Å) with decreased lattice mismatch of 7.4%. The information on the phase transition was primarily obtained indirectly by electron diffraction[8,9] and coaxial impact collision ion scattering spectroscopy.[10] Since these studies are based on macroscopic techniques averaging large sample areas, a supplementary STM study with high spatial resolution is helpful for further understanding of the details of the growth and the phase transition at 4 ML.

Thin Sn films exhibit very interesting electronic structures and physical properties, such as thickness-dependent oscillation of superconducting transition temperature for polycrystalline films deposited at 15 K on glazed alumina substrate[11] and thickness-modulated electronic structure for α-Sn films on CdTe substrates.[12,13] These results were interpreted in terms of quantum size effects (QSEs) due to the carrier confinement in thin films.[11–14] Since the film morphologies are unknown and sometimes ill defined in those studies, the evidence for QSE is more or less speculated.

In the present study, we have systematically investigated the growth and electronic structure of Sn deposited on $2\sqrt{3}$ surface at various temperatures by using STM/scanning tunneling spectroscopy (STS). The spatially resolved STM/STS enables a direct comparison between the morphologies, electronic structure, and, thus, the QSE. A structure transition from α-Sn to β-Sn at 4 ML and thickness-dependent striplike modulation structures from 4 to 11 ML due to symmetry difference and lattice mismatch and the preferential thicknesses of Sn islands due to QSE are identified. Annealing of the as-deposited films leads to a metal-insulator transition and a band-gap shift with respect to the Fermi energy for *n*- and *p*-type Si substrates. We show that the interesting growth behavior and electronic structure change in Sn films can be explained by the QSE under the Bohr–Sommerfeld quantization model.

II. EXPERIMENT

The details of the experimental setup and the procedures for clean Si(111)-7×7 surface preparation have been described elsewhere.[15] Unless otherwise indicated specifically, most experiments were performed on a *p*-type Si(111) wafer with a resistivity of 500 mΩ cm. Sn (99.999%) was deposited at a flux rate of 1 ML/min. The $2\sqrt{3}$ surface was ob-

tained by depositing 2 ML Sn on the Si(111) substrate held at 720 K. Sn was then deposited on the $2\sqrt{3}$ substrate at room temperature and various low temperatures (95, 150, 200, and 250 K). For room temperature annealing, the samples were transferred from the STM stage (80 K) to a room temperature sample holder, while for annealing at 285 K the samples were held on a manipulator at 285 K precooled by liquid nitrogen in distribution chamber. All STM images were acquired at 80 K with a constant tunneling current of 100 pA.

III. RESULTS AND DISCUSSION

A. Surface morphologies and thickness-dependent surface structures

Figures 1(a)–1(c) show typical STM images of the as-deposited samples with 5 ML Sn on $2\sqrt{3}$ surface at substrate temperatures of 200, 250, and 300 K (room temperature), respectively. Figure 1(d) shows the image acquired after the sample shown in Fig. 1(a) was annealed at room temperature for 3 h, while Fig. 1(e) shows that after the sample shown in Fig. 1(b) was annealed at 285 K for 1 h. The corresponding line profile is shown below each STM image. Flat-top Sn islands and disordered wetting layer between islands are observed in all these images, and a typical Stranski–Krastanov growth is suggested. The layer numbers of Sn islands above the wetting layer are calculated with the β-Sn(100) surface distance of 2.92 Å,[10] and preferential thicknesses of odd-numbered layers (5 and 7 ML) are identified. Most islands are 5 ML (1.46 nm) high, while others are 7 ML (1.76 nm) high. Besides the common observation that islands increase in size at the cost of decreasing density and are arranged along the upper Si terrace edges [the steps are indicated by dotted lines in Figs. 1(c)–1(e)] with either increasing substrate temperature or annealing time [comparing Figs. 1(c)–1(e) to Figs. 1(a) and 1(b)], it is interesting to note that the preferential thicknesses of islands are always 5 and 7 ML. This thickness preference is caused by QSE, which will be discussed in Sec. II.

Uniform films were expected to be achieved at a lower substrate temperature and higher coverage.[16–18] Therefore, deposition was performed at a lower substrate temperature and then annealing at room temperature. Figure 1(f) shows the image of the as-deposited sample with 15 ML Sn at 150 K. Large flat-top wedge-shaped islands crossing several terraces are formed.[19] Figure 1(g) shows the morphology at a nominal thickness of 30 ML deposited at 95 K. A flat film with 1 ML thickness variation is obtained. However, the 30 ML Sn film cannot survive at room temperature and breaks into islands of various thicknesses [see Fig. 1(h)] after 1 h room temperature annealing. In summary, the epitaxy of Sn on the $2\sqrt{3}$ surface is a typical Stranski–Krastanov growth with flat-top islands on the wetting layer. The Sn islands exhibit preferential thicknesses of odd-numbered layers. No uniform films are observed at room temperature.

The surface structures of Sn islands were carefully investigated. Figures 2(a)–2(f) show high resolution STM images taken on islands with different thicknesses. A striplike feature between hexangular and parallelogram structures with a periodic separation of about 3 nm is observed on the surface of 4 ML island, as shown in Fig. 2(a). In Fig. 2(b), the two structures are labeled by rectangle and ellipse; the unit cells are also outlined. When the thickness is higher than 4 ML, only parallelogram structures are observed, as shown in Figs. 2(c)–2(f) and the zoom-in images in Fig. 3 (in Fig. 3, the surface unit cells are outlined).

The observation above indicates that a phase transition from α-Sn to β-Sn occurs at 4 ML. Most parallelogram structures are about 4.2 ± 0.3 Å long with angles varying from 80° to 89°. The fact that θ is not 90° suggests a structure distortion during the transition, as the buried α-Sn remains stabilized at the interface even after the formation of β-Sn on it.[9] Moreover, a striplike modulation along the diagonal direction of the unit cells of Sn overlayers [see Figs. 3(a)–3(d) for the orientation relationship between unit cells and the striplike modulation] arises, which turns out to be very sensitive to thickness. For instance, the surface of 5 ML island consists of regular strips with an average separation of 4 nm [Fig. 2(c)], which increases to 5, 6, and 9 nm for 7 ML [Fig. 2(d)], 8 ML [Fig. 2(e)], and 10 ML [Fig. 2(f)], respectively. It becomes weaker with increasing thickness and disappears at 11 ML [see Fig. 3(b) for the image of 11 ML island]. Importantly, this striplike modulated structure is independent of the bias voltage used for imaging. An exception is the 8 ML island whose image is bias dependent, as shown in Figs. 3(c) and 3(d) for different sample biases of 0.8 and 0.4 V. Since 8 ML is an unstable thickness, the bias-dependent behavior implies an electronic effect. Nevertheless, the major STM observations of the distorted and modulated surface structures of the islands and their insensitivity on bias voltage can be best explained by the strain effect or the strain relaxation, which seems to complete at 11 ML. It is worth mentioning that after a room temperature annealing of these samples for several hours, no apparent change was observed in the surface structure. However, STS spectra near zero bias show different behaviors upon annealing, which will be discussed in Sec. III.

B. Thickness-dependent quantum well states and their correlation with morphologies

Since the electronic wave functions normal to the plane of the islands are modified by the imposed boundary formation (the Sn surface and the Sn/Si interface), standing wave states and/or QWSs will be formed. The corresponding density of states displays a stepwise increase with energy, which should be detectable with STS. The I-V spectra should appear stepwise[19] and the dI/dV-V spectra should exhibit a series of peaks at the onset of a new emerging subband.[20] Generally, the QWS energy is inversely proportional to the square of the island thickness; therefore, the spectra are characterized by a series of thickness-correlated peaks.

Figures 4(a)–4(c) display the dI/dV-V spectra taken on the as-deposited wedge-shaped islands from 7 to 19 ML [see Fig. 1(f) for the topography image]. The Fermi level is located at zero bias. Down-pointing arrows mark the onset of the highest occupied quantum well states (HOQWSs) and up-pointing arrows mark the lowest unoccupied quantum well states (LUQWSs), which are the first peaks just below

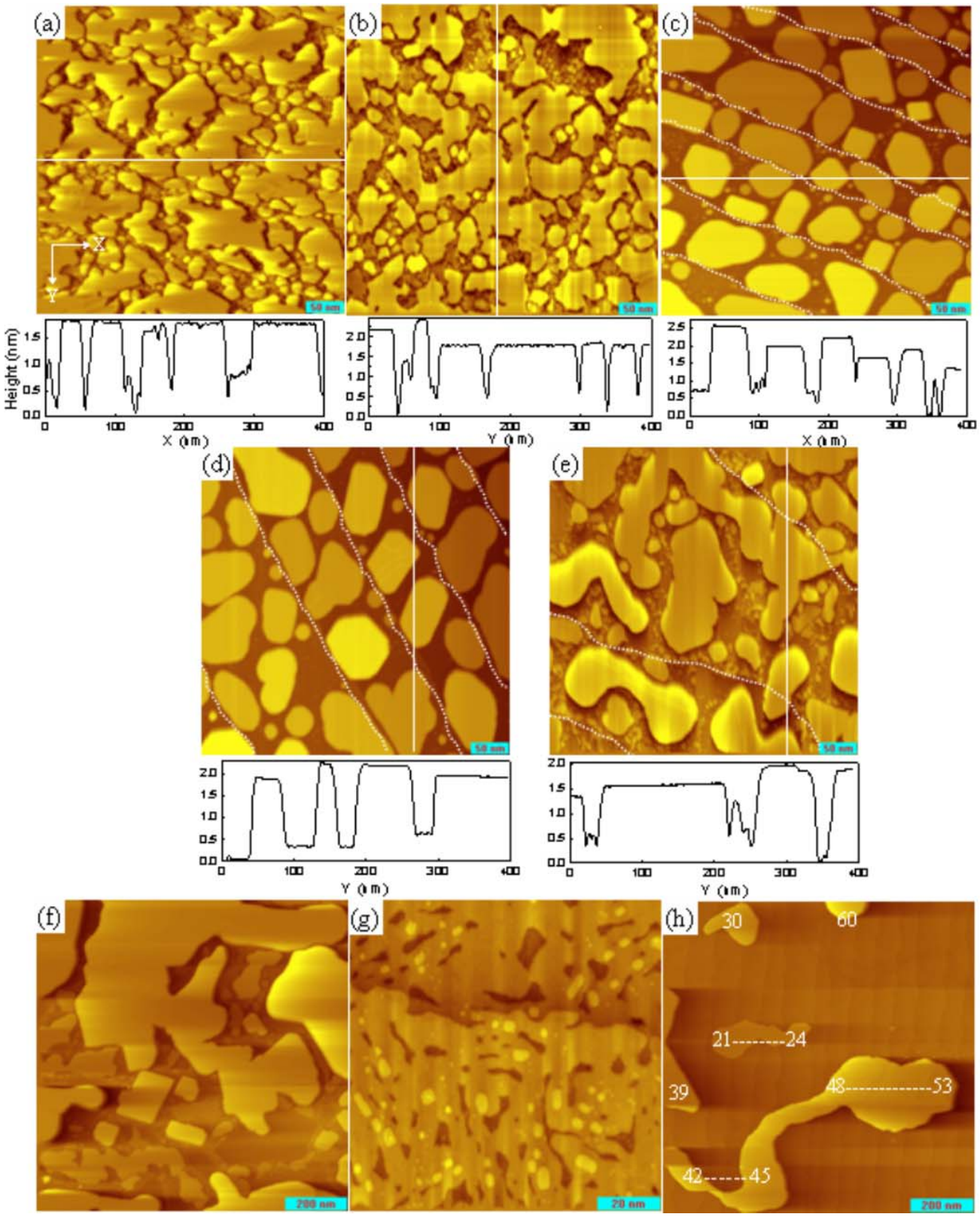

FIG. 1. (Color online) STM images of the films after Sn was deposited on the Si(111)-$2\sqrt{3}$ surface at various substrate temperatures. [(a)–(c)] (400×400 nm^2) 5 ML Sn deposited at 200, 250, and 300 K, respectively; (d) (400×400 nm^2) after the sample shown in (a) was annealed at room temperature for 3 h; (e) (400×400 nm^2) after the sample shown in (b) was annealed at 285 K for 1 h; (f) (1000×1000 nm^2) 15 ML Sn deposited at 150 K; (g) (100×100 nm^2) 30 ML Sn deposited at 95 K; (h) (1000×1000 nm^2) after the sample shown in (g) was annealed at room temperature for 1 h. The line profile corresponding to the white line is shown just below each image. The numbers in (h) indicate the thicknesses of islands in the unit of ML.

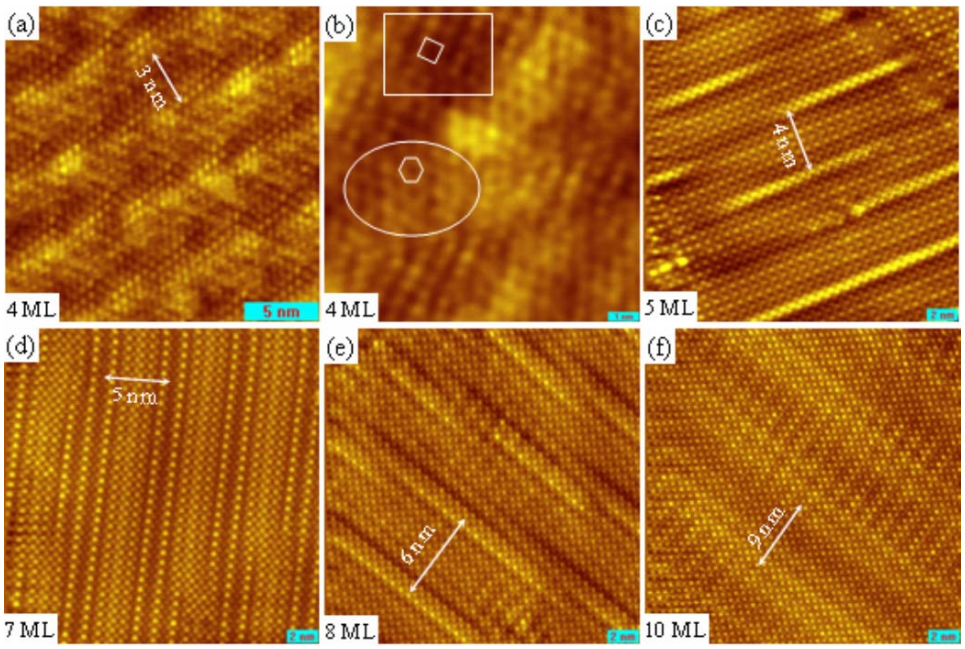

FIG. 2. (Color online) High resolution STM images acquired on islands of various thicknesses: [(a) and (b)] 4 ML, (c) 5 ML, (d) 7 ML, (e) 8 ML, and (f) 10 ML. (e) was acquired at a sample bias of 0.8 V, while others at 0.4 V. Except for (b) (10×10 nm^2) which is zoomed from (a) showing the details of the coexisting hexangular and tetragonal structures, other images are 20×20 nm^2. The double-arrowed lines indicate the periods of the striplike features caused by strain.

and above the Fermi level, respectively. The dotted line indicates the middle position between the HOQWS (E_{HOQWS}) and LUQWS (E_{LUQWS}). The shift of the middle positions with thickness is clearly evidenced. Define the distance from the middle position between E_{HOQWS} and E_{LUQWS} to the Fermi level as $\delta=(E_{\mathrm{HOQWS}}+E_{\mathrm{LUQWS}})/2-E_F$. δ also exhibits a bilayer oscillation, as described in the plot of δ versus island thickness in Fig. 4(d). The fact that the absolute δ values for the odd-numbered (7, 9, and 11 ML) islands are much smaller than those even-numbered (8, 10, and 12 ML) islands suggests that the odd-numbered layers should have a higher surface charge density than their counterparts, which in turn makes the surface energy of the odd-numbered islands lower.[20–22] This is the reason why most islands in Figs. 1(a)–1(e) are 7 ML. We also note that there is an even-odd film stability transition at 12 ML and a Fermi level crossing of QWSs at 17 ML.

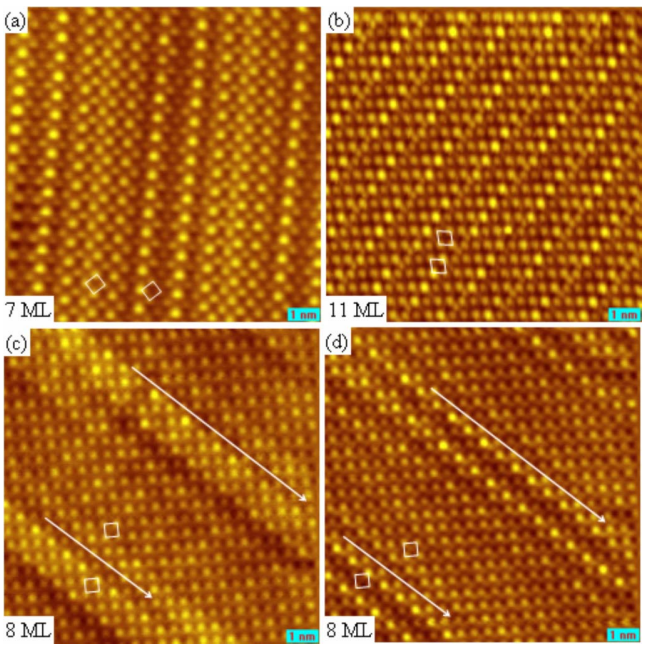

FIG. 3. (Color online) High resolution STM images (10×10 nm^2) acquired on islands of various thicknesses: (a) 7 ML, (b) $\geq$11 ML, and [(c) and (d)] 8 ML. (c) was acquired at a sample bias of 0.8 V, while others at 0.4 V. The unit cells are outlined by parallelograms. The arrowed lines in (c) and (d) show the area where the feature distinctly changes with bias.

Regardless of some reports for QSE,[11–13] the QWSs observed here provide the first direct evidence for QSE in the Sn/Si(111) system. The band structure of Sn(100) exhibits an energy band crossing the Fermi level,[23] while that of Si(111) exhibits a gap of about 0.7 V (it changes with doping).[24] So, QWSs can be formed in this system as long as sharp surface and interface boundaries are formed. The Fermi wavelength (λ_F) along the (100) direction for the β-Sn crystal is 3.88 Å.[25] With the interlayer spacing $d_0=2.92$ Å, we have $2d_0=3\lambda_F/2$, which implies that every bilayer growth of Sn can accommodate three new bound electronic states. Based on the Bohr–Sommerfeld quantization rule,[26] the calculated QWS oscillation period should be 2 ML, which is exactly observed here. Since the transition from α-Sn to β-Sn occurs at 4 ML and Sn islands are strained, the interlayer spacing is not the exact bulk value of 2.92 Å, which can explain the even-odd transition mentioned above.

Next, we discuss why the film as thick as 30 ML cannot survive at room temperature. It has been widely accepted that the stability of an epitaxial film on a substrate of a different

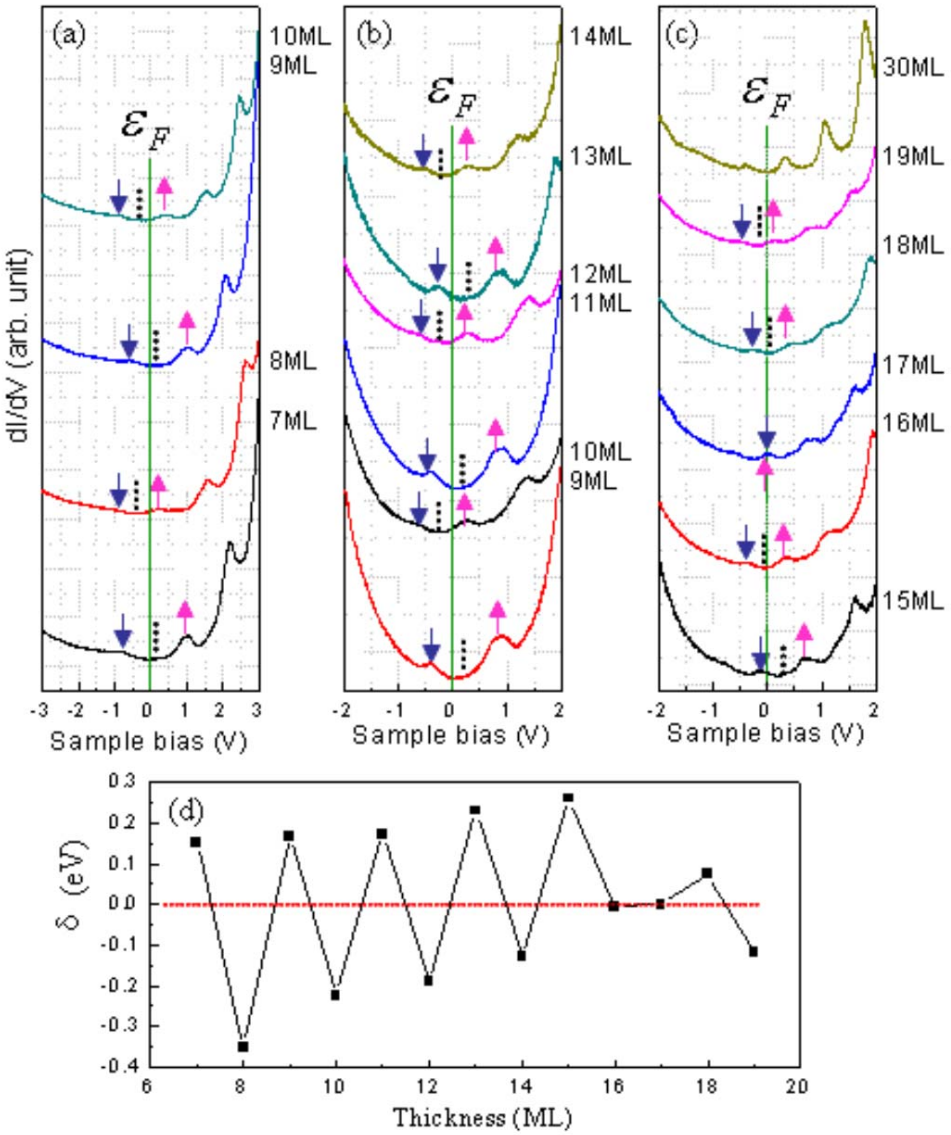

FIG. 4. (Color online) [(a)–(c)] Series dI/dV-V spectra taken from islands of various thicknesses as deposited at 150 K. For comparison, the STS spectrum for the as-deposited 30 ML film at 95 K is shown in (c). The HOQWSs are marked with down-pointing arrows and the LUQWSs are marked with the up-pointing ones. The dotted line marks the middle position between the HOQWS and the LUQWS. (d) The energy separation from the middle position of the HOQWS and the LUQWS to the Fermi level as a function of island thicknesses. All the spectra were obtained at 0.4 V and 100 pA.

material is primarily determined by the competition between surface tension and stress. For the epitaxial growth of metal on semiconductor substrate, three other competing factors, QSE, charge spilling, and interface induced Friedel oscillations, are responsible for the stability of metal films.[27] Under far-from-equilibrium conditions, QSE driven atomic flat metal film growth on semiconductor substrates can be obtained, such as Ag on GaAs(110) (Ref. 16) and Pb (Ref. 17)/Al (Ref. 18) on Si(111). As a characteristic of the QSE-facilitated stability of metal films on semiconductor substrates, the critical thickness, at which uniform flat thin films can be formed and stabilized, is determined by the balance between the long range force induced by QSE and the elastic force induced by lattice mismatch.[16–18] Furthermore, the critical thickness increases with increasing substrate temperature since a new balance needs to be reestablished by energy gain from QSE at increasing thickness to compensate the energy penalty from the elastic force accumulated from the increase of the film volume and/or due to thermal annealing resulted lattice expansion.[17,28]

The STS spectrum of the 30 ML film [see Fig. 1(g) for the topography image] is shown in Fig. 4(c), and QWSs are observed, which indicates that the QSE still takes effect at such thickness. The film cannot survive at room temperature and breaks into isolated islands [Fig. 1(h)]. This is different from the QSE modulated growth mentioned in previous studies. For example, uniform Pb films thicker than 10 ML formed at low temperature remain stable at room temperature with an atomically flat surface that is partially covered by 2 ML islands.[17] Accordingly, either uniform film of 30 ML or

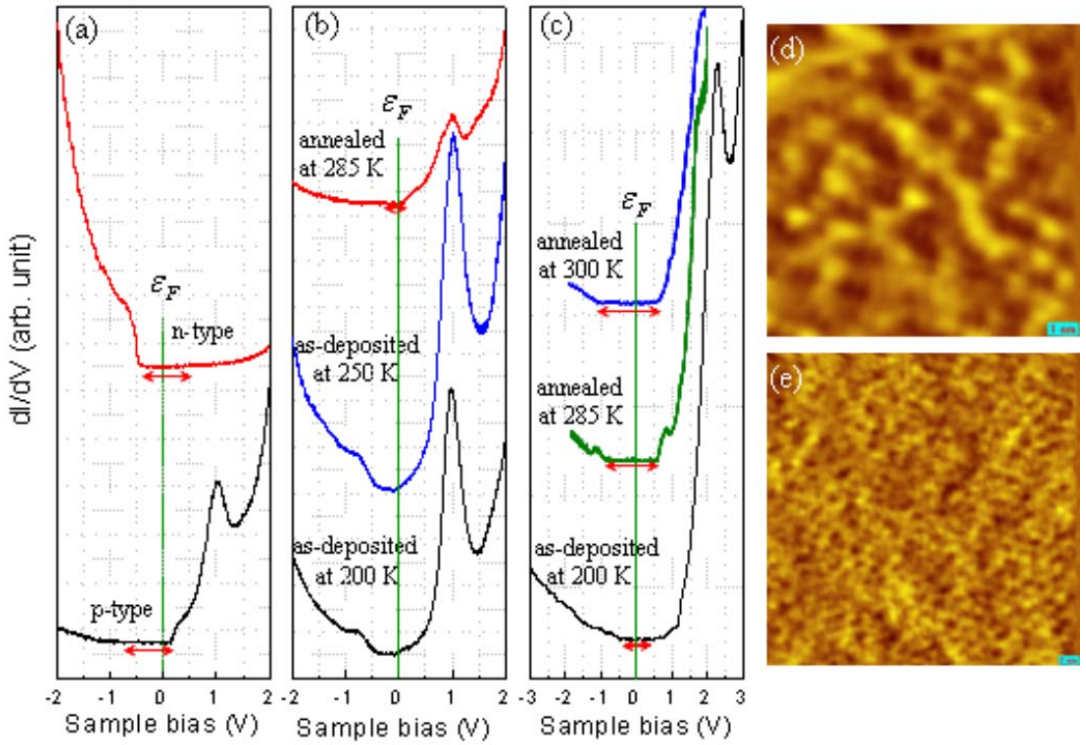

FIG. 5. (Color online) A series dI/dV-V spectra taken from (a) the 5 ML island deposited at 200 K and annealed at room temperature for 3 h on n-type and p-type Si, (b) the 5 ML islands, and (c) the wetting layers. (d) a 10×10 nm^2 STM image of the wetting layer acquired at 1.5 V and (e) a 30×30 nm^2 STM image acquired on the 5 ML island at −1.0 V. The band gaps are labeled by double-arrowed lines. The spectra were obtained at (a) 0.7 V, 100 pA, (b) 0.5 V, 100 pA, and (c) 1.0 V, 10 pA. No obvious change was observed in the spectra recorded at different setpoints.

film of 29 ML half covered by 2 ML islands should be formed after annealing, depending on whether 30 ML is the preferred thickness or not. One possible reason for the instability is the charge spilling, i.e., the electron transfer between the Sn overlayer and the Si substrate, which leads to an attractive force between the Sn/Si interface and the Sn surface and destabilizes the flat films, while the interface induced Friedel oscillation in electron density only imposes oscillatory modulation onto QSE and charge spilling effect.[27] The important role of charge spilling at the interface in determining the stability of films has been convincingly shown in that it induces a change in the preferred height with different substrates.[29]

C. Change in electronic property induced by annealing

Figure 5(a) shows two STS spectra of the 5 ML island deposited at 200 K and annealed at room temperature for 3 h [the lower one is for the p-type Si and the top one is for the n-type Si; its morphology is shown in Fig. 1(d)]. Band gaps are clearly observed in both spectra. Furthermore, the band gaps are asymmetric with regard to the Fermi level and shift opposite to the direction which should be determined by the doping of Si substrates. For example, the band gap of the p-type Si(111) substrate should shift to positive bias as a result of the Fermi level shifting to the valence band, while the spectrum stretches from −0.6 to 0.1 V, which shifts to negative bias. On the other hand, the band gap of the n-type Si(111) substrate should shift to negative bias. Again, the spectrum stretching from −0.3 to 0.5 V shifts to positive bias.

In order to understand the results, STS measurement was performed on as-deposited and annealed samples at various growth and/or annealing temperatures. The main results are as follows. First, annealing leads to the opening of band gaps and opposite shifting of the spectra on Sn islands. The three curves in Fig. 5(b) (from bottom to up) show the spectra of 5 ML island as deposited at 200 K, as deposited at 250 K, and then annealed at 285 K for 1 h, respectively [see Figs. 1(a), 1(b), and 1(e) for the corresponding topography images]. Band-gap opening (with a gap from −0.15 to 0.08 V) was only observed for the sample annealed at 285 K, which shifts oppositely. Second, for the wetting layers, annealing leads to band-gap opening and opposite shift, as shown in Fig. 5(c) [see Fig. 5(d) for the topography image of the wetting layer]. Different from the results on Sn islands, the same direction shifting of the band gap as that of the Si substrate is observed on the as-deposited wetting layer at 200 K, while annealing oppositely shifts the band gaps of the wetting layers. As summarized in Table I, the band gaps shown in Fig. 5(c) are 0.70 V (from −0.25 to 0.45 V, in the same shift direction as that of p-type Si), 1.07 V (from −0.56 to 0.51 V, the shifting direction is opposite to that of the p-type Si), and 1.71 V (from −1.11 to 0.60 V, shifting further upon room temperature annealing). The two peaks in the middle of the spectrum are probably from the tip states since they are not reproduc-

TABLE I. Energy band gaps measured from the spectra of wetting layers formed at different deposition and annealing conditions.

	As deposited at 200 K	Annealed 1 h at 285 K	Annealed 3 h at 300 K
Gap starting point (V)	−0.25	−0.56	−1.11
Gap ending point (V)	0.45	0.51	0.60
Gap value (V)	0.70	1.07	1.71

ible. The peak at 2.2 V in the lower spectrum may correspond to some quantized state of the clusters in the wetting layer because peaks at 2.2 ± 0.2 V are usually observed. In summary, for the annealed samples, band-gap opening and opposite shifting either on the Sn islands or on the wetting layers take place, while for the as-deposited samples, band-gap opening only occurs on the wetting layers and the gaps shift in the same direction as those of the Si substrates. 250–285 K is found to be a temperature window, within which not only does band-gap opening occur for islands [the top curve in Fig. 5(b)] but also the band gap of the wetting layer oppositely shifts [the middle curve in Fig. 5(c)].

The appearance of band gaps of the Sn islands seems to be a reflection of electron transfer at the Sn-Si interface rather than some substantial electronic structure change in Sn islands themselves. First, it is not a semiconductor-metal transition in bulk Sn. The metal-semiconductor transition after annealing at 285 K is opposite to the characteristic transition from semiconducting α-Sn to metallic β-Sn that occurs at 13.2 °C. Also, the observed band-gap values are different from those of α-Sn.[12] Although below 11 ML the surface structures are thickness dependent, the parallelogram β-Sn is the only possible phase above 4 ML, which further rules out the possibility of the β-Sn to α-Sn transition. Second, it cannot be a Wilson-type transition. In this case, it should work for both the islands and the wetting layer. Third, the bias range in which samples can be imaged by STM changes with the area percentage of the wetting layer, which indicates the effect of the wetting layer to the STM scanning. The larger the area percentage of the wetting layer and the thinner the Sn islands, the larger the sample bias is required. Finally, band-gap opening on Sn islands is consistent with the fact that the gap of the wetting layer oppositely shifts even within the same critical temperature window from 250 to 285 K. The features seen in Fig. 5(e) (topography image acquired on the 5 ML island at −1.0 V) are quite different from those observed in Figs. 2 and 3, which were recorded at smaller bias. They reflect the Sn/Si interface structure due to nondiffractive electron scattering, as previously reported in Pb/Si system.[30] Based on the result, we believe that the electronic structure change in the Sn islands is a reflection of that in the buried wetting layer rather than the substantial change in the Sn islands themselves.

Although both Si and Sn are tetravalent and share the same electronegativity, theoretical calculations predicted an energy gap of 0.25 V between Sn-like filled states and Si-like empty states, which was supported by inverse photoemission results; the charge transfer from Si to Sn associated with the formation of a semiconductor gap at E_F was verified as well.[31] Furthermore, the direct space x-ray standing wave imaging technique clearly revealed that a significant fraction of the Sn atoms substituted for the Si atoms in the bottom of the Si surface bilayer during annealing.[32] So, it is thus reasonable to assume that the increase and opposite shift of band gaps of the wetting layers upon annealing should be related to the electron transfer (Sn-Si intermixing) in the wetting layer (at the interface). This assumption is consistent with the discussion in the second section that the charge spilling change after annealing might destabilize and break down the uniform films formed at low temperature. To verify this assumption, further theoretical calculation is necessary.

IV. SUMMARY

The morphologies and electronic structure of Sn thin films prepared on Sn induced Si(111)-$2\sqrt{3}$ substrates have been studied by STM/STS. Due to the large lattice mismatch and symmetry difference, the transition from α-Sn to β-Sn occurs at 4 ML, and the surface exhibits thickness-dependent striplike modulation structures from 4 to 11 ML. The formation of QWSs and the change in electron transfer in the wetting layer (at Sn-Si interface) with annealing are identified by STS. The former modulates the surface energy and induces the thickness preference of Sn islands, while the latter leads to the breaking of the uniform films prepared at low temperature.

ACKNOWLEDGMENT

This work was supported by the National Science Foundation and Ministry of Science and Technology of China.

*Corresponding author; xcma@aphy.iphy.ac.cn

[1] J. M. Carpinelli, H. H. Weitering, M. Bartkowiak, R. Stumpf, and E. W. Plummer, Phys. Rev. Lett. **79**, 2859 (1997).
[2] R. Cortés, A. Tejeda, J. Lobo, C. Didiot, B. Kierren, D. Malterre, E. G. Michel, and A. Mascaraque, Phys. Rev. Lett. **96**, 126103 (2006).
[3] R. I. G. Uhrberg, H. M. Zhang, T. Balasubramanian, S. T. Jemander, N. Lin, and G. V. Hansson, Phys. Rev. B **62**, 8082 (2000).
[4] S. K. Ramchurn, D. M. Bird, and D. W. Bullett, J. Phys.: Condens. Matter **2**, 7435 (1990).
[5] X. F. Lin, I. Chizhov, H. A. Mai, and R. F. Willis, Appl. Surf. Sci. **104/105**, 223 (1996).
[6] C. Törnevik, M. Hammar, N. G. Nilsson, and S. A. Flodström, Phys. Rev. B **44**, 13144 (1991).
[7] L. Ottaviano, G. Profeta, L. Petaccia, C. B. Nacci, and S. Santucci, Surf. Sci. **554**, 109 (2004).
[8] D. T. Wang, N. Esser, M. Cardona, and J. Zegenhagen, Surf. Sci.

343, 31 (1995).
[9] B. Roldan Cuenya, M. Doi, and W. Kenue, Surf. Sci. **506**, 33 (2002).
[10] J. T. Ryu, M. Katayama, and K. Oura, Surf. Sci. **515**, 199 (2002).
[11] B. G. Orr, H. M. Jaeger, and A. M. Goldman, Phys. Rev. Lett. **53**, 2046 (1984).
[12] S. Takatani and Y. W. Chung, Phys. Rev. B **31**, 2290 (1985).
[13] Li-Wei Tu, George K. Wong, and John B. Ketterson, Appl. Phys. Lett. **55**, 1327 (1989).
[14] B. I. Craig and B. J. Garrison, Phys. Rev. B **33**, 8130 (1986).
[15] L. L. Wang, X. C. Ma, P. Jiang, Y. S. Fu, S. H. Ji, J. F. Jia, and Q. K. Xue, Phys. Rev. B **74**, 073404 (2006).
[16] A. R. Smith, K.-J. Chao, Q. Niu, and C. K. Shih, Science **273**, 226 (1996).
[17] Y. F. Zhang, Z. Tang, T. Z. Han, J. F. Jia, and Q. K. Xue, Surf. Sci. **596**, L331 (2005).
[18] Hong Liu, Y. F. Zhang, D. Y. Wang, M. H. Pan, J. F. Jia, and Q. K. Xue, Surf. Sci. **571**, 5 (2004).
[19] I. B. Altfeder, K. A. Matveev, and D. M. Chen, Phys. Rev. Lett. **78**, 2815 (1997).
[20] W. B. Su, S. H. Chang, W. B. Jian, C. S. Chang, L. J. Chen, and Tien T. Tsong, Phys. Rev. Lett. **86**, 5116 (2001).
[21] F. K. Schulte, Surf. Sci. **55**, 427 (1976).
[22] C. M. Wei and M. Y. Chou, Phys. Rev. B **66**, 233408 (2002).
[23] G. Weisz, Phys. Rev. **149**, 504 (1966).
[24] C. Tserbak, H. M. Polatoglou, and G. Theodorou, Phys. Rev. B **47**, 7104 (1993).
[25] C. Kittel, *Introduction to Solid State Physics* (Wiley, New York, 1966).
[26] P. M. Echenique and J. B. Pendry, J. Phys C **11**, 2065 (1978); N. V. Smith and C. T. Chen, Surf. Sci. **247**, 133 (1991).
[27] Z. Y. Zhang, Q. Niu, and C. K. Shih, Phys. Rev. Lett. **80**, 5381 (1998).
[28] Zhigang Suo and Zhenyu Zhang, Phys. Rev. B **58**, 5116 (1998).
[29] V. Yeh, L. Berbil-Bautista, C. Z. Wang, K. M. Ho, and M. C. Tringides, Phys. Rev. Lett. **85**, 5158 (2000).
[30] I. B. Altfeder, D. M. Chen, and K. A. Matveev, Phys. Rev. Lett. **80**, 4895 (1998).
[31] A. Charrier, R. Pérez, F. Thibaudau, J.-M. Debever, J. Ortega, F. Flores, and J.-M. Themlin, Phys. Rev. B **64**, 115407 (2001); J. Lobo, A. Tejeda, A. Mugarza, and E. G. Michel, *ibid.* **68**, 235332 (2003).
[32] A. A. Escuadro, D. M. Goodner, J. S. Okasinski, and M. J. Bedzyk, Phys. Rev. B **70**, 235416 (2004).